

WIDEBAND RECONFIGURABLE LOG PERIODIC PATCH ARRAY

M. R. Hamid^{1, *}, P. S. Hall², and P. Gardner²

¹Fakulti Kejuruteraan Elektrik, Universiti Teknologi Malaysia (UTM), Johor Bahru Campus, Johor 81310, Malaysia

²Electronic Electrical and Computer Engineering, University of Birmingham, B15 2TT, UK

Abstract—This paper presents a novel wideband to narrow band reconfigurable log periodic aperture coupled patch array. The wide to narrow band reconfiguration is realized by closing a selected group of slot apertures, to deactivate the corresponding group of patches. The patches are fed with a modulated meander line through aperture slots. A wideband mode from 7–10 GHz and three selected narrow band modes at 7.1, 8.2 and 9.4 GHz are demonstrated. Potentially, the number of sub bands can be increased or decreased as can the bandwidth of the sub bands by selecting a specific number of active elements. To verify and demonstrate the proposed design method, a prototype has been developed with ideal switches. Very good agreements between the measured and simulated results are presented.

1. INTRODUCTION

The increasing need for multiband radio front ends has led to research on frequency reconfigurable antennas [1–4]. Wide to narrow band reconfigurable antennas have received attention [5–7], as they offer multi-functionality and are potentially important for future cognitive radio systems which employs wideband sensing and reconfigurable narrowband communications. Ideally, the system needs narrow band communication that can be reconfigured to any specific desired band. However, most reported wide to narrow band antennas have a limited number of switched narrow band operation and fixed in bandwidth. To overcome this, we propose a novel wideband log periodic patch array with a capability to switch into a desired narrow band mode.

Received 30 August 2012, Accepted 29 October 2012, Scheduled 1 November 2012

* Corresponding author: Mohamd Rijal Hamid (rijal@fke.utm.my).

Log periodic antennas have multiple elements, which resonate in a log periodic fashion. Using this property, a frequency reconfigurable log periodic antenna is proposed. Recently, work on reconfigurable log periodic antennas has been reported. In the log periodic dipole array described in [5], ideal switches are used to control each pairs of dipole arm of the antenna. This can switch from a wideband of 1–3 GHz, to several narrow bands. Similar work on this has also been reported in [8–10]. In contrast to wide to narrowband reconfiguration, work in [11–14] demonstrates band notch method for log periodic antennas. In this paper a novel log periodic antenna with the potential for switched band functionality to operate in a wideband or narrowband mode is presented. The antenna is an aperture coupled patch array with meandered feed. The feed has modulation to prevent a structural stop bands similar to that used in log periodic monopole array [15]. The antenna reconfiguration is realized by inserting switches into the slot aperture of the structure. In the array demonstrated here the switches are formed by metal sections, of the same size as a switch, bridging the slot aperture. A wide bandwidth mode is demonstrated from 7.0–10 GHz and three narrowband modes at 7.1, 8.2 and 9.4 GHz can be formed. A prototype has been manufactured. Measured results show good performance of the proposed designs. The proposed antenna is designed to operate from 7–10 GHz. A wider bandwidth can be obtained using more elements. Potentially, the number of sub bands can be increased or decreased, as can the bandwidth of the sub bands by selecting a specific number of active elements. Details of the proposed design are described. Section 2 discusses the advantages in choosing an aperture coupled log periodic patch array as a candidate for reconfiguration. Sections 3 and 4 discuss the problem of the structural stop band and the procedure for eliminating it. The fabricated antenna is discussed in Section 5. Finally the results are presented in Sections 6 (simulations) and 7 (measurements) and follow by conclusions in Section 8. Some preliminary results of this work were presented in [16].

2. MOTIVATION

The criteria defining the best reconfigurable design, such as the number of switches used to reconfigure the structure and the design simplicity, are investigated here. For that purpose, the structure of the log periodic printed dipole array Fig. 1(a) [5], an electromagnetic coupled patch array Fig. 1(b) [17] and an aperture coupled patch array Fig. 2 [16] are compared. Potentially, the aperture coupled log periodic patch array (LPA) is a good candidate. The configuration,

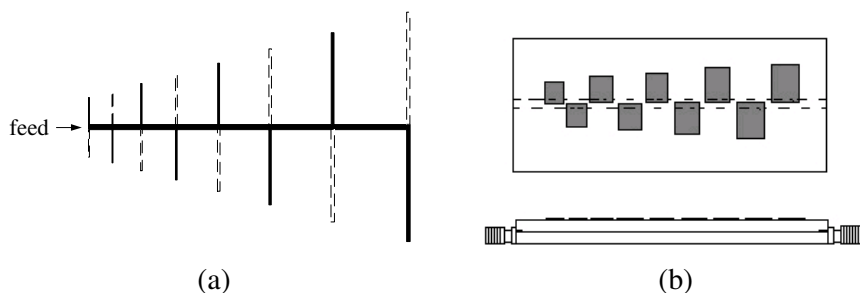


Figure 1. (a) Log periodic printed dipole array [8]. (b) An electromagnetic coupled patch array [15].

allows each radiating element to be controlled using one switch, thus, offering fewer switches compared to the dipole array [5]. This thus reduces the problems of biasing many switches. Furthermore, biasing for the switches can be located within the ground plane and therefore coupling to radiation will be limited. Application of dc bias is believed to be hard in a log periodic printed dipole array and has not been demonstrated yet. On the other hand, an electromagnetic coupled structure such as reported by [17] will be very hard to switch because there is no specific coupling mediator between the patch and the feed line, unlike the aperture slot as proposed here.

3. STRUCTURAL STOP BAND IN APERTURE COUPLED ARRAYS

To achieve a broadside direction, the feeding phase of an array should be set to 0° or 360° . However, in a series fed array, this gives rise to high input VSWR. To reduce VSWR, the feeding phase is set to be less or more than 360° , which then produces a beam angle in a forward or back fire direction. In this array, the condition for forward fire at $\theta = 0^\circ$ can be met when the phasing between elements, β , is 270° . The distance between array elements in free space, σ is set to 0.25λ . This is obtained from equation [18], $\beta = -k\sigma \cos \theta$ with $k = 2\pi/\lambda$ and θ is defined as in Fig. 5(a).

Figure 2 shows the configuration of the log periodic aperture coupled patch array. The excess length, d , between adjacent elements is determined by β . For $\beta = 270^\circ$, $d = 0.75\lambda_g$. If d is greater than half a wavelength, attenuation below the resonant frequency will occur [19], due to a structural stop band, which will cause high VSWR at the input. To understand the structural stop band completely the

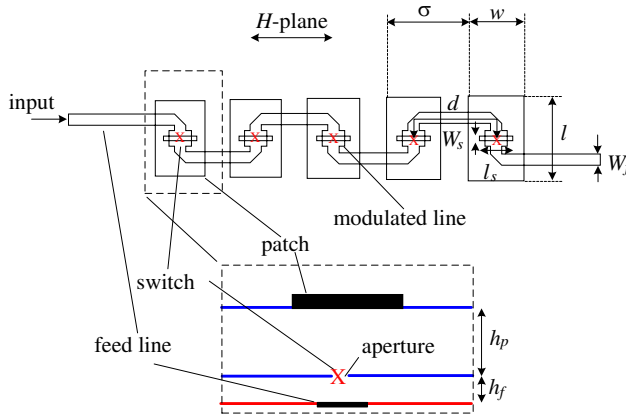


Figure 2. Log periodic aperture coupled patch array, w_f — feed line width, h_f — feed line substrate thickness, h_p — patch substrate thickness, d — excess length, σ — free space spacing, w — patch width, l — patch length, w_s — aperture width, l_s — aperture length [Dimensions: $h_f = 0.787$ mm, $h_p = 0.254$ mm, rohacell = 2 mm, $d_1 = 16.1$ mm, $\sigma = 15.86$ mm, $w_1 = 7$ mm, $l_1 = 10.77$ mm, $w_f = 2.38$ mm, $\epsilon_r = 2.2$ (for h_f and h_p)], scaling factor $\tau = 1.02$.

dispersion data and the image impedance of each of the cells of the log periodic structure are examined. Detailed explanations of this have been reported in [19].

4. ELIMINATING STRUCTURAL STOP BAND

A cascade of single cells forming a log periodic structure, loaded by shunt loads, with an expansion factor, τ , is shown in Fig. 3. If each cell has at least one structural stop band, a limited bandwidth of $< 2 : 1$ array will result. To overcome this, the variation of image impedance must be minimized. The image impedance of a short section of line is defined as the terminating impedance on the output port which leads to an input impedance that has the same value. A method suggested in [19] for minimizing the variation of image impedance is applied here. It is achieved when the impedance of the line is modulated as shown in the left side of Fig. 3. The line is modulated by changing the characteristic impedance of a small part of the line, where the modulated part has a width, w_{f1} and a length d_1 . The excess length, d now is $d = 0.5d_2 + d_1 + 0.5d_2$. By way of example, a two port representing a single element of the structure, resonating at 9.583 GHz,

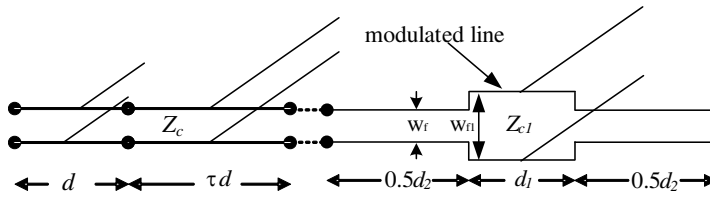


Figure 3. A cascaded single cells forming a log periodic structure.

with d is $0.75\lambda_g$, is simulated to examine the image impedance and dispersion. The image impedance is given by [20], as $Z_i = \sqrt{\frac{B}{C}}$ where B and C are the parameters of the $ABCD$ matrix for the cell. The attenuation is given by, $ad = \cosh^{-1} |\gamma d|$ where $\gamma d = (a + jb)d$ is the propagation constant and a and b is attenuation and phase constant respectively. Fig. 4(a) shows the calculated image impedance, which is very different from 50 ohms between 6.65 and 7.84 GHz before modulation for a case where $d_1 = 0$ mm. This causes a stop band between those frequencies, as shown in Fig. 4(b). The magnitude of the image impedance at this frequency is 31Ω , Fig. 4(a). To eliminate the stop band, the line width of the modulated part, w_{f1} , Fig. 3 is set to 4.7 mm, to give an impedance of 31Ω . d_1 is then optimised until the variation of the image impedance is minimised. In this example, d_1 is found to be 2.2 mm. The image impedance for $d_1 = 2.2$ mm is also shown in Fig. 4(a). The variation of image impedance is now small and has a value of 44.3Ω at the resonant frequency. The attenuation plot shows ad is very small, from 0 to 12 GHz. This method is applied for each element that produces a stop band within the operating frequency of 7–10 GHz.

5. RECONFIGURABLE LOG PERIODIC APERTURE COUPLED PATCH ARRAY DESIGN

In this section, the design of the log periodic array antenna is described. Fig. 5 shows the proposed structure with 20 radiating elements. The smallest element (patch 1) is $w_1 = 7$ mm and $l_1 = 10.77$ mm. The aperture width, w_{s1} is 0.8 mm and aperture length, l_{s1} is 5.85 mm. An expansion factor of 1.02 is used. The patches are printed on a 0.254 mm thick Duroid 5880 substrate, with a dielectric constant of 2.2. The meandered 50Ω feed line and slot apertures are etched on a similar 0.787 mm thick substrate. The array is terminated in a matched load to prevent reflections. Each aperture is spaced a quarter wavelength apart and fed with 270° phasing thus give a forward fire radiation

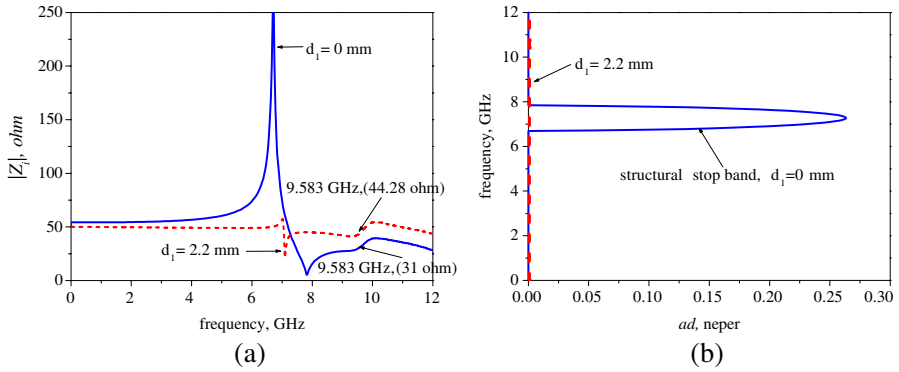


Figure 4. (a) Image impedance, $|Z_i|$. (b) Attenuation, ad .

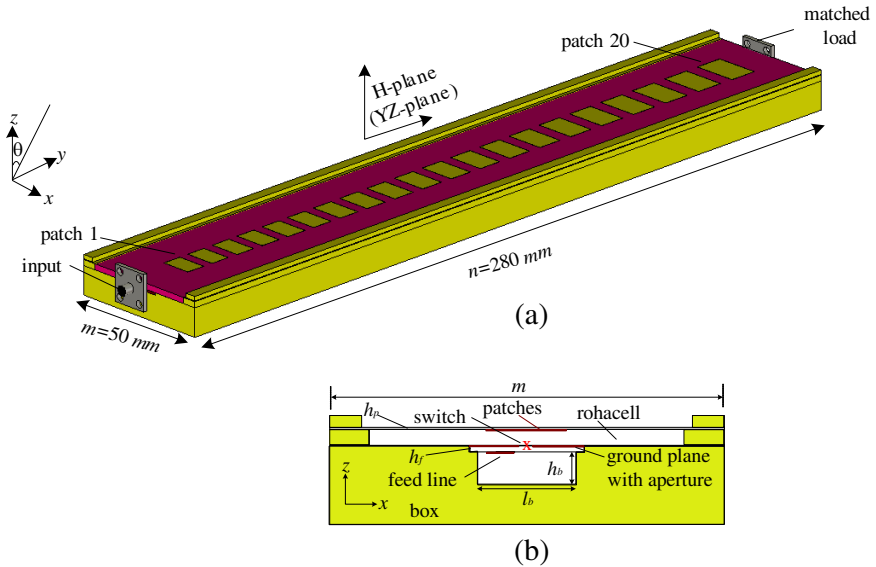


Figure 5. Proposed antenna structure. (a) Perspective view. (b) Side view. $\tau = 1.02$, $\epsilon_r = 2.2$ (for h_f and h_p), $\epsilon_r = 1.09$ (for rohacell), $w_f = 2.38$ mm, $h_f = 0.787$ mm, $h_p = 0.254$ mm, rohacell = 2 mm, $d_1 = 16.1$ mm, $\sigma = 15.86$ mm, $w_1 = 7$ mm, $l_1 = 10.77$ mm.

pattern. A single switch, denoted as ‘ x ’ (see Fig. 5(b) and Fig. 2), is placed at the centre of each aperture. Rohacell foam, with a dielectric constant of 1.09 and thickness of 2 mm, is sandwiched between the patch and feed substrates. The patch configuration is arranged in

the H -plane axis. The feed line is enclosed with a screening box size of $h_b \times l_b$, which is important to reduce back radiation. The box size (h_b is 4.18 mm and l_b is 12.7 mm) is designed so that the cut off frequency is at 11.8 GHz which is above the top end operating band of 10 GHz. In the simulation, metal pads, of size 1 mm \times 1 mm, have been used to approximate switching devices. The presence of the metal pad represents the switch ON state and absence represents the OFF state. This is believed acceptable to demonstrate the basic concept. For a twenty element LPPA, twenty switches are employed. Wideband operation is achieved when all the switches are in the OFF state thus making the antenna act as a normal log periodic antenna. To demonstrate narrow band operation, such as in a high band mode, four of the highest frequency slots were kept open. The rest of the slots

Table 1. Switches location.

No of Slot	Wideband	High band	Mid band	Low band
1	X	X	-	-
2	X	X	-	-
3	X	X	-	-
4	X	X	-	-
5	X	-	-	-
6	X	-	-	-
7	X	-	-	-
8	X	-	X	-
9	X	-	X	-
10	X	-	X	-
11	X	-	X	-
12	X	-	X	-
13	X	-	X	-
14	X	-	-	-
15	X	-	-	-
16	X	-	-	X
17	X	-	-	X
18	X	-	-	X
19	X	-	-	X
20	X	-	-	X

x, OFF states (open); -, ON states (closed)

were closed by bridging them with the switches. The other sub bands are achieved by bridging a group of slots of the antenna as shown in Table 1. The design has been simulated using CST simulation software.

6. SIMULATION RESULTS

In this section, simulation results are first presented to demonstrate the concepts. The simulated wideband mode scattering parameter and the simulated efficiency is shown in Fig. 6(a) and Fig. 6(b) where efficiency is defined as $1 - |S_{11}|^2 - |S_{21}|^2$. The antenna operates over a frequency range of 7 to 10 GHz with efficiency ranging from 70 to 95%. Fig. 7 shows the effects on the radiation patterns. It is observed there is strong back radiation from the feed line when the box surrounding the feed line is absent. The back radiation is effectively reduced after the screening box is in place.

Figure 8 shows the simulated efficiency of the reconfigurable array in the four frequency bands. It shows that some degree of frequency reconfiguration can be achieved, with wide, high, mid and low bands clearly seen, corresponding to the switched patch groups. There are, however, ripples in the various narrow bands which are very pronounced in the low frequency band. There are some features of the design that might account for this. There is a change in the impedance seen by the feed line when the switch is short circuited. This will reintroduce a structural stop band within the low band and this might be responsible for some of the ripples. Also, higher order modes in the patches are believed to give rise to patch excitation outside the

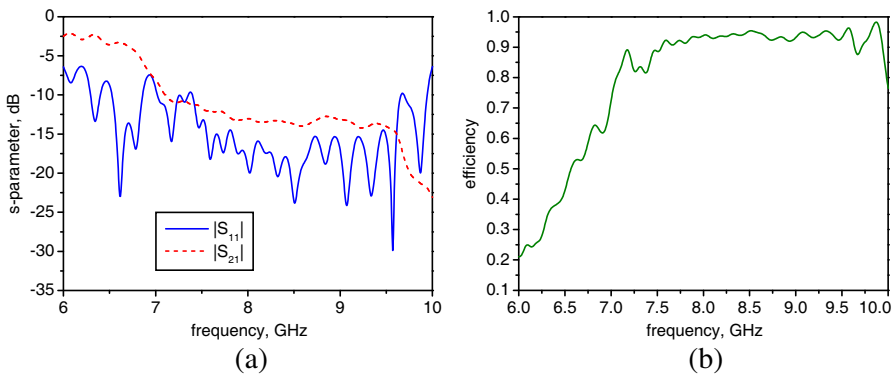


Figure 6. Simulated wideband mode. (a) Scattering parameters. (b) Efficiency.

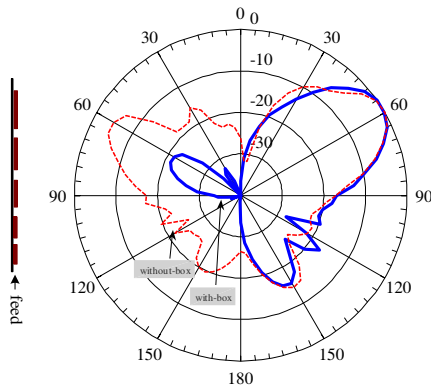


Figure 7. Simulated effects of screening box on radiation pattern (H -plane) excited at 8.2 GHz, with and without screening box.

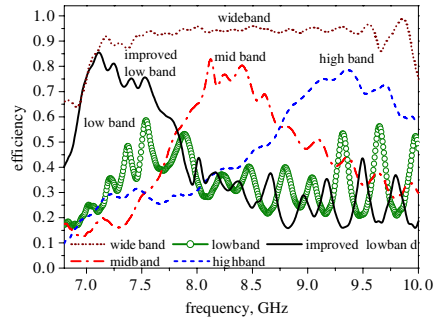


Figure 8. Simulated efficiency for selected four frequency bands.

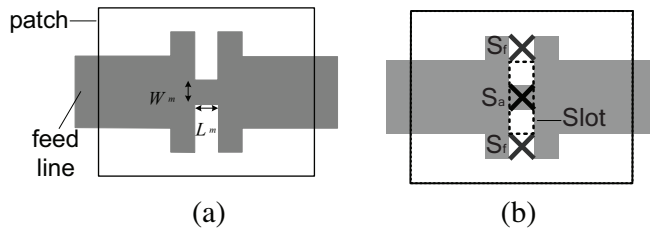


Figure 9. (a) Modified feed line and (b) modified switch configuration, S_f — switch on feed, S_a — switch on slot.

desired band [21]. A slight drop in efficiency in the narrow band mode is expected because fewer patches are excited.

As noted above, when the slot is short circuited, there is a change in the impedance seen by the feed line. This is presumably because the inductive part of the feed line equivalent circuit and slot is reduced, changing the image impedance. To compensate for the change and to eliminate the stop band, the modulated line section has a slot across it, as shown in Fig. 9(a), with a small pad connecting the left and the right part of the line at the centre. This configuration is believed to restore the equivalent inductance in the structure when the slot is short circuited. To simplify the design process, L_m is set equal to the slot aperture width. By choosing the W_m appropriately, the variation

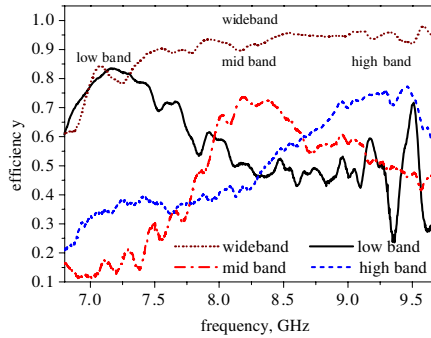


Figure 10. Measured efficiency of four selected band of the proposed reconfigurable log periodic patch array.

Table 2. Gain of the proposed antenna.

Wideband Gain, dBi	7.1 GHz	8.2 GHz	9.4 GHz
Simulated	11.64	13.60	13.08
Measured	9.83	16.42	14.54

Narrowband Gain, dBi	7.1 GHz	8.2 GHz	9.4 GHz
Simulated	10.91	10.74	10.61
Measured	8.08	13.69	11.56

of image impedance can be minimised and the structural stop band eliminated. The improvement of low band mode efficiency can be seen in Fig. 8.

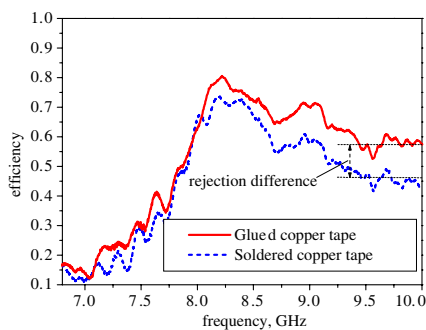
In addition, it was found necessary to modify the switch configuration to that shown in Fig. 9(b) in order to maintain the performance of the other bands. Two switches, S_f , are added to slots in the feed line. The feed line switches, S_f , are open when the aperture switch, S_a , is closed. On the other hand, the S_f switches are closed when the S_a switch is open, to keep reasonably similar performances in the other modes. Wideband and improved low band results of Fig. 8, are with the S_f and S_a switches present. The gain in each band is shown in Table 2 and discussed in the next section.

7. MEASUREMENT RESULT

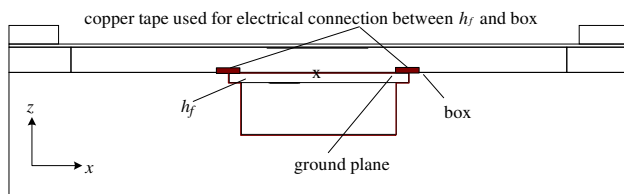
The measured efficiency is presented in Fig. 10. In the wideband mode, the antenna operates over a frequency range of 7 to 10 GHz with

efficiency ranging from 80–95%. The figure also shows the measured efficiency of the reconfigurable LPA for each selected three frequency bands. In the low band mode, the measured efficiency at mid and high frequencies is higher than the simulated, suggesting that less out of band rejection is being achieved. Similarly, in the mid band mode the measured efficiency at higher frequencies is higher than in the simulation, again suggesting reduced rejection. This may be accounted for by improper shielding between h_f substrate and the box. Leakage from the gap between the ground plane and the box was found to be a significant problem which was solved by improving the electrical connection between the two. Fig. 11(a) shows that a better rejection out of band in the mid band mode is achieved if the copper tape is soldered to the substrate and the box as shown in Fig. 11(b).

The measured and simulated H -plane radiation patterns for the wideband mode excited at 7.1 GHz, 8.2 GHz and 9.4 GHz are shown in Fig. 12. Good agreement and well behaved radiation patterns are obtained. The measured and simulated H -plane radiation patterns for the narrowband modes are presented in Fig. 13. Good agreement and well behaved radiation patterns are also obtained. It is observed that



(a)



(b)

Figure 11. (a) Out of band rejection in mid band mode. (b) Proposed screening box where a copper tape is used to reasonably enclose the lower substrate, h_f into the shielding box.

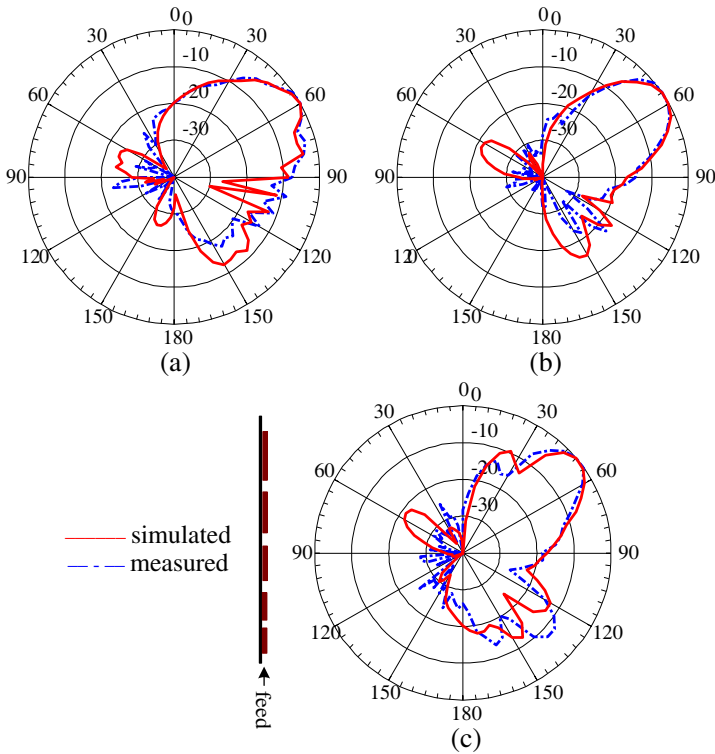


Figure 12. Wideband mode radiation pattern excited at (a) 7.1 GHz, (b) 8.2 GHz and (c) 9.4 GHz.

the beam in the wideband mode is tilted more toward the forward fire direction as the frequency increases, which is presumably due to the increasing length of the active region at higher frequency. Finally, the gain of the wideband mode and narrowband mode are shown in Table 2. The values are lower in the narrow band modes. This is due to the wide beamwidth as shown in Fig. 13 compared to Fig. 12. This indicates that in the wideband mode the active region is bigger than in the narrowband case. The differences trend between simulated and measured gain values for wideband and narrowband cases are nearly similar suggest that the differences maybe due to small tolerances during measurement setup.

An array with real switches such as pin diodes could be implemented by following the described design guideline. However the off and on state model of the diode and decoupling components

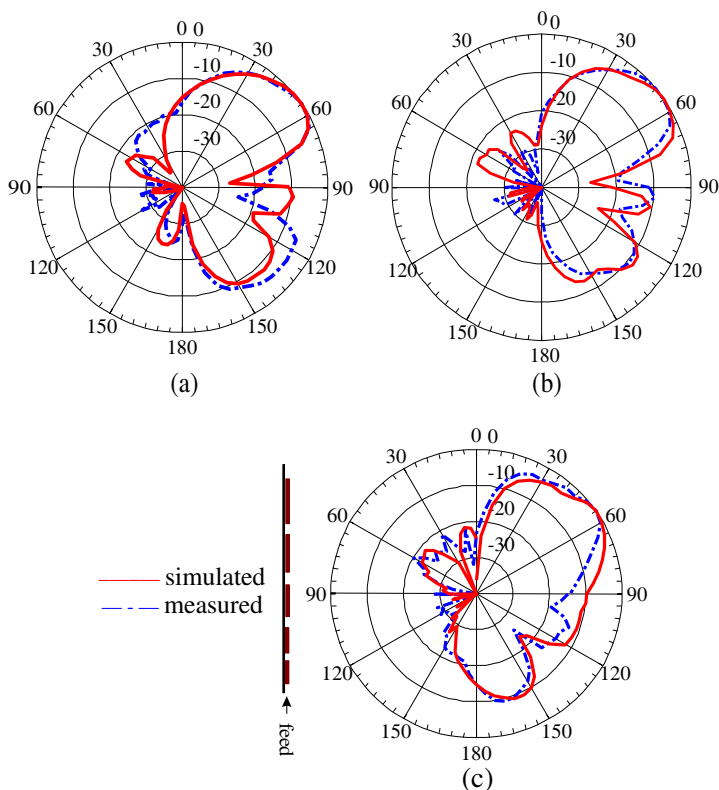


Figure 13. Narrow band mode radiation pattern. (a) Low band mode excited at 7.1 GHz. (b) Mid band mode excited at 8.2 GHz and (c) high band mode excited at 9.4 GHz.

should be included in all calculations. In the demonstration described here, these were not included. While using real switches, dc line and decoupling component must be included in the design. The bias circuit can be implemented in the ground plane which will help to reduce coupling to radiation. The biasing can be designed where each switch is controlled independently. Fig. 14 shows the proposed biasing. The ground plane can be DC isolated into few sections with for example 0.3 mm width slots. To preserve RF continuity, SMD capacitors (DC blocker) can be used to bridge the slots. Therefore the diodes can be forward biased appropriately with DC voltage.

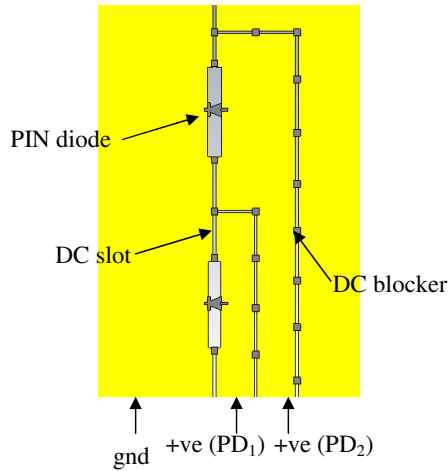


Figure 14. Proposed biasing circuit.

8. CONCLUSIONS

A novel reconfigurable log periodic patch array has been proposed by inserting switches within the aperture slots coupling the patches to the feed line. A wideband mode and three narrow band modes of reconfiguration are demonstrated, when groups of patches were selected within the array. A design guideline has been derived to allow some optimizing of the low band performances. More sub-bands could be achieved with different patches group selection. Nevertheless, in the relatively simple example shown good efficiency has been obtained for each of the sub bands. The antenna is low profile and can be easily mounted to any structure such as in the body of an aircraft. Furthermore the bias circuit can be implemented easily in the ground plane which will help to reduce coupling to radiation. However there are some drawbacks. Ideally there should be only one single switch needed to switch off one element, but because of the reintroduction of the stop band in the low band mode, two extra switches are needed to improve the performance. Therefore additional loss resulting from switches is incurred. The need for a feed line screening box also makes the structure relatively complex. However the demands of future radio systems are so great, that any pre-filtering from the antenna may be welcomed by systems designers. Therefore, the proposed antenna could be a suitable solution for applications requiring wideband sensing and dynamic band switching, particularly in very wideband cognitive radio or in military applications.

ACKNOWLEDGMENT

This work is funded in part by EPSRC, grant reference number: EP/FOI 7502/1. The authors are also grateful to the Universiti Teknologi Malaysia (UTM) for Ph.D. sponsorship for M. R. Hamid.

REFERENCES

1. Costa, F. and A. Monorchio, "Design of subwavelength tunable and steerable Fabry-Perot/leaky wave antennas," *Progress In Electromagnetics Research*, Vol. 111, 467–481, 2011.
2. Ramadan, A. H., K. Y. Kabalan, A. El-Hajj, S. Khoury, and M. Al-Husseini, "A reconfigurable U-koch microstrip antenna for wireless applications," *Progress In Electromagnetics Research*, Vol. 93, 355–367, 2009.
3. AbuTarboush, H. F., et al., "Reconfigurable tri-band H-shaped antenna with frequency selectivity feature for compact wireless communication systems," *IET Microwaves Antennas & Propagation*, Vol. 5, 1675–1682, November 18, 2011.
4. Han, T. Y. and C. T. Huang, "Reconfigurable monopolar patch antenna," *Electronics Letters*, Vol. 46, 199-U22, February 4, 2010.
5. Mirkamali, A. and P. S. Hall, "Wideband frequency reconfiguration of a printed log periodic dipole array," *Microwave and Optical Technology Letters*, Vol. 52, 861–864, 2010.
6. Tawk, Y. and C. G. Christodoulou, "A new reconfigurable antenna design for cognitive radio," *IEEE Antennas and Wireless Propagation Letters*, Vol. 8, 1378–1381, 2009.
7. Ghanem, F., et al., "Switched UWB to narrowband planar monopole antenna," *2010 Proceedings of the Fourth European Conference on Antennas and Propagation (EuCAP)*, 1–3, April 12–16, 2010.
8. Gheethan, A. A. and D. E. Anagnostou, "The design of reconfigurable planar log-periodic dipole array (LPDA) using switching elements," *IEEE Antennas and Propagation Society International Symposium, APSURSI'09*, 1–4, June 1–5, 2009.
9. West, D. N. and S. K. Sharma, "Frequency reconfigurable compact multiband quasi-log periodic dipole array (QLPDA) antenna for wireless communications," *2010 IEEE Antennas and Propagation Society International Symposium (APSURSI)*, 1–4, July 11–17, 2010.
10. Ismail, M. F., et al., "Wideband to narrowband frequency

- reconfiguration using PIN diode,” *Microwave and Optical Technology Letters*, Vol. 54, 1407–1412, June 2012.
11. Yu, C., et al., “Ultrawideband printed log-periodic dipole antenna with multiple notched bands,” *IEEE Transactions on Antennas and Propagation*, Vol. 59, 725–732, March 2011.
 12. Mruk, J. R., et al., “Band rejection methods for planar log-periodic antennas,” *IEEE Transactions on Antennas and Propagation*, Vol. 58, 2288–2294, 2010.
 13. Chen, S.-Y., et al., “Uniplanar log-periodic slot antenna fed by a CPW for UWB applications,” *IEEE Antennas and Wireless Propagation Letters*, Vol. 5, 256–259, 2006.
 14. Lin, G., et al., “A band-notched UWB log-periodic dipole antenna fed by strip line,” *IEEE International Conference on Ultra-Wideband (ICUWB)*, Vol. 1, 1–4, September 20–23, 2010.
 15. Green, P. B. and P. E. Mayes, “50-Ohm log-periodic monopole array with modulated-impedance microstrip feeder,” *IEEE Transactions on Antennas and Propagation*, Vol. 22, 332–334, 1974.
 16. Hamid, M. R., et al., “Frequency reconfigurable log periodic patch array,” *Electronics Letters*, Vol. 46, 1648–1650, December 9, 2010.
 17. Hall, P. S., “Multioctave bandwidth log-periodic microstrip antenna array,” *IEE Proceedings H on Microwaves, Antennas and Propagation*, Vol. 133, 127–136, 1986.
 18. Balanis, C. A., *Antenna Theory: Analysis and Design*, 3rd Edition, A John Wiley and Sons Inc. Publication, 2005.
 19. Ingerson, P. and P. Mayes, “Log-periodic antennas with modulated impedance feeders,” *IEEE Transactions on Antennas and Propagation*, Vol. 16, 633–642, 1968.
 20. Pozar, D. M., *Microwave Engineering*, 2nd Edition, Wiley, Chichester, New York, 1998.
 21. Hall, P. S., et al., “Reconfiguration of Vivaldi and log periodic antennas,” *Proc. Allerton Antenna Symposium*, September 22–23, 2009.